Supporting Information

Superweak Coordinating Anion as Superstrong Enhancer of Cyanine Organic Semiconductor Properties

Donatas Gesevičius, Antonia Neels, Sergii Yakunin, Erwin Hack, Maksym V. Kovalenko, Frank Nüesch, and Jakob Heier*

Table of Contents

General Information

General Notation for this Work

- Two symmetrical indolenine derivatives connected with a pentamethine chain

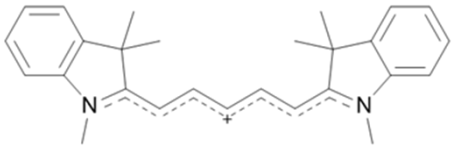

2-[5-(1,3-dihydro-1,3,3-trimethyl-2H-indol-2-ylidene)-1,3-pentadien-1-yl]-1,3,3-trimethyl-3H-indolium (Cy5)

- Superweak coordinating anion

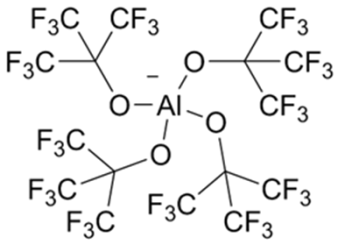

Tetrakis(nonafluoro-*tert*-butoxy)aluminate $[Al(pftb)_4]^-$

- Abbreviation for the dye used in this work

Cy5[Al(pftb)$_4$]

Figure S1. Overview of the used notation of the compound for this work.

Anion Exchange Procedure

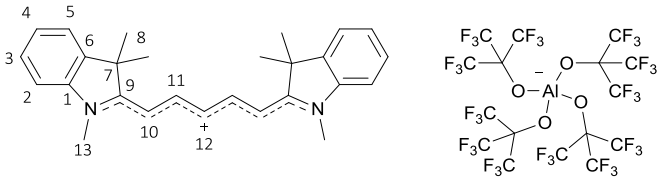

1.00 g, (1.03×10^{-3} mol) Lithium tetrakis(nonafluoro-*tert*-butoxy)aluminate and 0.43 g 2-[5-(1,3-dihydro-1,3,3-trimethyl-2H-indol-2-ylidene)-1,3-pentadien-1-yl]-1,3,3-trimethyl-3H-indolium chloride were dissolved in 100 mL chlorobenzene. The mixture was stirred overnight followed by 1 h of ultra-sonication at room temperature. After filtration and evaporation of all volatile compounds the reaction yielded 1.38 g of a blue powder.

$[C_{43}H_{30}AlF_{36}N_2O_4]$ 1349.65 g mol^{-1}

^{1}H NMR (400 MHz, Chloroform-*d*) δ: 7.79 (dd, J = 13.5, 12.6 Hz, 2H, H(11)), 7.44 (m, 2H, H(3)), 7.41 (d, 2H, J = 8.4 Hz, H(5)), 7.29 (td, J = 7.5, 0.9 Hz, 2H, H(4)), 7.12 (d, J = 7.8 Hz, 2H, H(2)), 6.46 (t, J = 12.5 Hz, 1H, H(12)), 6.03 (d, J = 13.6 Hz, 2H, H(10)), 3.55 (s, 6H, H(13)), 1.70 (s, 12H, H(8)) ppm.

^{13}C NMR (101 MHz, Chloroform-*d*) δ: 173.9 (C9), 153.2 C(11), 142.5 (C1), 140.8 (C6), 129.1 (C3), 126.1 (C4), 125.1 (C12), 122.9 (C5), 121.3 (q, J = 293 Hz, CF_3), 110.6 C(2), 103.2 (C10), 79.0 (bp, $C(CF_3)_3$), 49.5 (C7), 31.1 (C13) 28.0 (C8) ppm.

^{19}F NMR (377 MHz, Chloroform-*d*) δ: -75.4 (s, 36F) ppm.

Crystal Structure

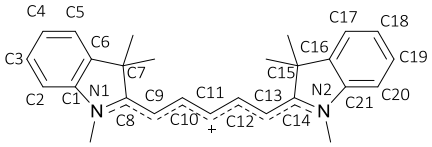

Figure S2. Cyanine atom numbering.

All crystal structures solutions and refinements were performed with common crystallographic software.[2,3]

Overview about possible ways to access parameters describing anion-cation interactions in a single crystal

Formula used to calculate the lattice energy:

Since the anions and cations are complex molecules built from several atoms the term cation/anion radii needs further specifications and assumptions. Additionally the positive and negative charges are delocalised over several atoms. Therefore the coordination distance determination between the cation and anion is not a trivial task.

One common disadvantage of usual methods is that the ions are treated as spherical objects. This assumption causes strong deviations from the real situation where the ions represent several covalent bound atoms of irregular shape.

A simple and reliable model was developed for complex molecular ions which translates the ionic radii into a molecular volume.[1] The molecular volume can be precisely calculated for any geometrical shape taking information from the X-Ray structural data.

$$\Delta U = |Z^+||Z^-|v\left(\frac{a}{V_m{}^{\frac{1}{3}}} + \beta\right)$$

ΔU = Lattice energy, $|Z^+||Z^-|$ = charge of cation/anion, v = number of ions per molecule, V_m = molecular volume, a = slope of the regression line: 117.3 kJ mol^{-1} nm (molecular volume against lattice energy of literature known salts), β = intercept of the regression line: 51.9 kJ mol^{-1} (molecular volume against lattice energy of literature known salts).

However, the presented equation for molecular volume can only be used when no intercalated solvents are present within the unit cell. In case of solvate crystals the estimation of molecular volumes becomes a non-trivial task. Olex[2] with implemented SHELXL[3] was used to squeeze all residual electron density assigned to solvent molecules. Subsequently the masked solvent volume was subtracted from the unit cell leading to a corrected unit cell volume. Finally the corrected unit cell volume was divided by coordination number yielding the molecular volume of the corresponding organic salts (**Table S1**).

Table S1. Lattice energy calculation of different Cy5 chromophore salts.

Parameters	**Anion**				
	^-O_3SMe	**^-O_3SPh**	**$^-O_3SPhMe$**	**^-TFSI**	**$[Al(pftb)_4]^-$**
a/nm	4.01284	1.70193	1.11894	1.17454	1.12248
α/(°)	(90)	(90)	(84.938)	(103.83)	(90)
b/nm	1.70323	2.80027	1.17926	1.28785	5.0171
	(135.969)	(103.218)	(83.146)	(105.068)	(100.661)

Parameters	Anion				
	$^{-}O_3SMe$	$^{-}O_3SPh$	$^{-}O_3SPhMe$	$^{-}TFSI$	$[Al(pftb)_4]^{-}$
β/(°)					
c/nm	3.80012	2.20323	1.68978	1.37737	1.0425
γ/(°)	(90)	(90)	(63.980)	(116.063)	(90)
Z	24	12	2	2	4
I	1	1	1	1	1
V_m/nm^3	0.609	0.663	0.675	0.726	1.279
E_L/kJ mol^{-1}	380.57	372.84	371.24	364.83	319.92

Overview about possible determination of Coulomb and lattice energy from single crystals:

Formula used to calculate electrostatic Coulomb interactions:

$$E_{Coulomb} = \frac{1}{4\pi\varepsilon\varepsilon_0} \cdot \frac{z^2 e^2}{r}$$

Z = ionic charge, r = shortest contact distance between cation and anion, ε_0 = vacuum permittivity, ε = relative permittivity of the material.

Since the original formula assumes spherical anions and cations, the shortest cation-anion contact distance variable leads to a strong deviation from real conditions in complex molecular organic ions. The cation-anion distance can be replaced by the molecular volume.

$$r = \left(\frac{V_m}{2I}\right)^{\frac{1}{3}}$$

This modification provides more realistic values for complex molecular ions.

Table S2. Coulomb energy calculations of different Cy5 chromophore salts.

Parameters	Anion				
	$^{-}O_3SMe$	$^{-}O_3SPh$	$^{-}O_3SPhMe$	$^{-}TFSI$	$[Al(pftb)_4]^{-}$
ε	3.53	3.53	3.53	3.46	3.24
ε_0/ F m^{-1}	8.854×10^{-12}	8.854×10^{-12}	8.854×10^{-12}	8.854×10^{-12}	8.854×10^{-12}
z	1	1	1	1	1
e/C	1.602×10^{-19}	1.602×10^{-19}	1.602×10^{-19}	1.602×10^{-19}	1.602×10^{-19}
r/nm	0.67	0.69	0.69	0.71	0.86
E_c/eV	0.61	0.59	0.59	0.58	0.52

Table S3. Anion influence on bond length (Å) of the chromophore polymethine chain. *Average of the difference between C-C bond lengths in the polymethine chain.

Atom	Bond length (Å)
N1-C8	1.3606
C8-C9	1.3847
C9-C10	1.3987
C10-C11	1.3757
C11-C12	1.3857
C12-C13	1.3787
C13-C14	1.3907
N2-C14	1.3566
BLA*	1.32

Table S4. Anion influence on bending of the chromophore skeleton and indolenium ring conformation measured with Mercury 3.8.

Atoms	Angle (°)
C13-C14-N2-C21	179.5(9)
C11-C12-C13-C14	174.9(7)
C1-N1-C8-C9	177.9(7)
C6-C7-C8-C9	178.3(7)
C8-C9-C10-C11	176.0(4)
C13-C14-C15-C16	178.8(4)

UV-Vis absorbance

To determine the molar extinction coefficient 5.34×10^{-4} mol L^{-1} ethanol stock solution of Cy5[Al(pftb)$_4$] was prepared. Subsequently solutions with eight different concentrations were prepared by diluting the stock solution (**Table S5**).

Table S5. Used concentrations for the generation of calibration points in UV-Vis.

Solution	Concentration (mol L^{-1})
	Cy5[Al(pftb)$_4$]
1	8.32×10^{-8}
2	1.81×10^{-7}
3	1.09×10^{-6}
4	1.32×10^{-6}
5	1.60×10^{-6}
6	2.17×10^{-6}
7	6.08×10^{-6}
8	1.20×10^{-5}

All measurements were performed in a 1 mm quartz glass cuvette using 99.8 % ethanol as reference for the baseline. The relative molar extinction coefficient was calculated by multiplying the slope of the resulting plot of concentration against absorbance intensity by 10.

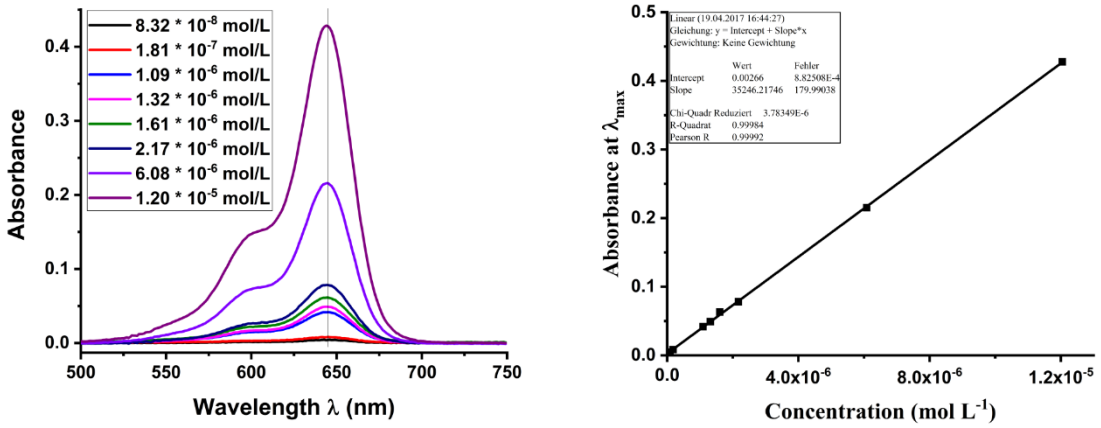

Figure S3. Concentration dependent absorbance and linear fit of the absorbance maxima against concentration.

The extracted optical data are summarized in **Table S6**. The optical band gap was calculated from the onset of the absorbance at higher wavelengths with the following equation.

$$E_{g(opt)} = \frac{h \times c}{\lambda_{onset}}$$

λ_{onset}: Onset of absorption band at higher wavelength, h: Planck constant, c: speed of light.

The oscillator strength describes the probability of a transition from a lower to an upper energy state. The higher the value the easier the electrons can be excited and the stronger absorbing is the dye.

$$f = 4.319 \times 10^{-9} \int \varepsilon(\upsilon)\, d\upsilon$$

$\varepsilon(\upsilon)$: Molar extinction coefficient as a function of wavenumber, υ: Wavenumber.

The whole absorbance peak was assumed to represent the full band of the lowest energy π-π^* transition and was integrated to calculate the oscillator strength.

First the wavelength was converted into wavenumbers with the following formula:

$$\upsilon = 1/(\lambda * 10^{-7})$$

Then the extinction coefficient was calculated for each wavenumber with the following formula:

$$\varepsilon_{(\upsilon)} = A/(c * d)$$

c: concentration in mol·L^{-1}, d: thickness of cuvette in cm, A: absorbance.

The calculations were performed for each recorded data point of the spectra.

Table S6. Calculated data from recorded UV-Vis spectra. * Onset energy at higher wavelengths obtained from EtOH solution.

Compound	ε_{max} (L mol^{-1} cm^{-1})	λ_{max} (nm)	λ_{onset} (nm)	$E_{(onset)}$* (eV)	f
Cy5[Al(pftb)$_4$]	3.52 ×10^5	644	674	1.83	1.48

Fluorescence

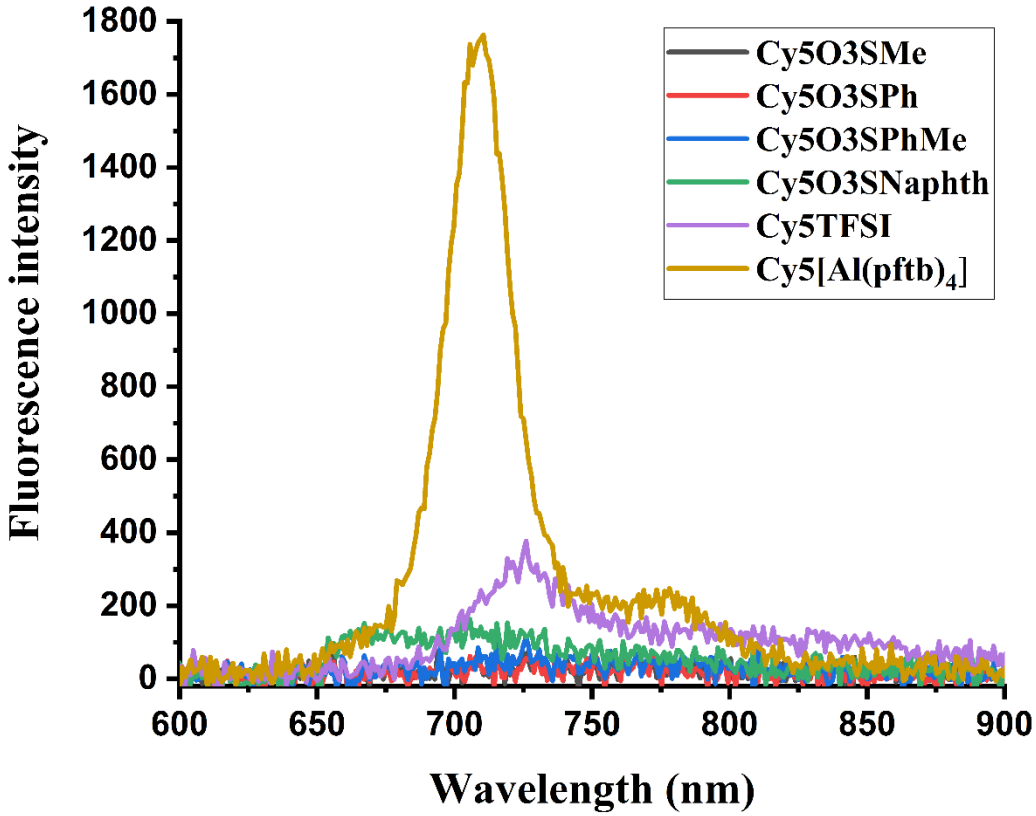

Figure S4. Fluorescence spectra obtained from 10 nm thick cyanine dye salt films spin-casted on hole transport layers MoO_3 (sulfonate and TFSI containing salts) and V_2O_5 (Cy5[Al(pftb)$_4$]).

Table S8. Quantum yield of cyanine films spin-cast on glass and hole transport layers. MoO_3 was used for sulfonate and TFSI containing salts while V_2O_5 was used for the salt containing the tetrakis(nonafluoro-*tert*-butoxy)aluminate anion.

Compound	Quantum yield on glass (%)	Uncertainty	Quantum yield on HTL (%)	Uncertainty
Cy5O$_3$SMe	4.77×10^{-2}	1.60×10^{-3}	4.74×10^{-4}	1.13×10^{-5}
Cy5O$_3$SPh	4.96×10^{-2}	2.10×10^{-4}	4.85×10^{-4}	3.82×10^{-5}
Cy5O$_3$SPhMe	5.17×10^{-2}	2.2×10^{-3}	4.82×10^{-4}	1.41×10^{-5}
Cy5O$_3$SNaphth	6.04×10^{-2}	3.90×10^{-3}	4.80×10^{-4}	6.85×10^{-5}
Cy5TFSI	9.09×10^{-2}	3.60×10^{-3}	6.19×10^{-4}	2.12×10^{-5}
Cy5[Al(pftb)$_4$]	3.26×10^{-1}	1.80×10^{-2}	1.25×10^{-3}	1.46×10^{-4}

Active Light Absorbing Layer Morphology

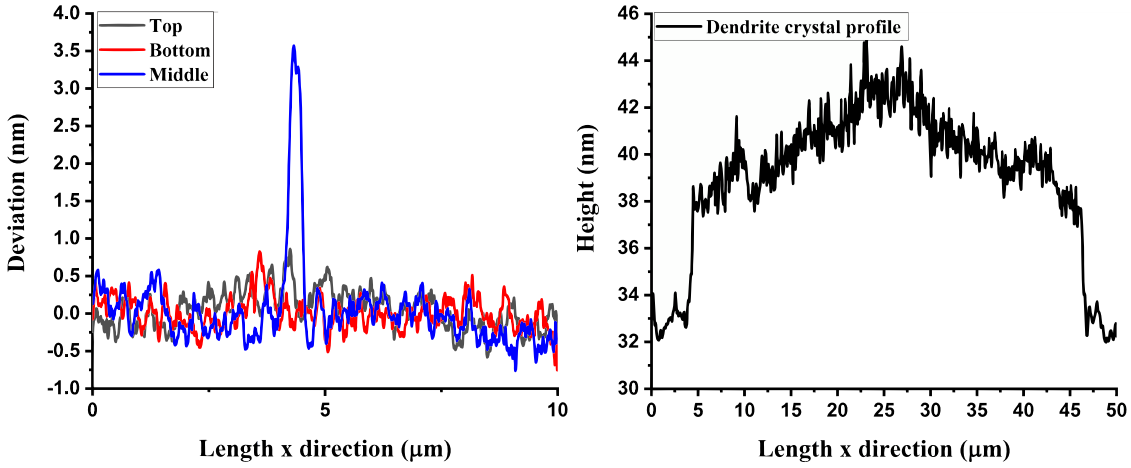

Figure S5. Left: Roughness profiles of the dye film coated on V_2O_5 hole transport layer extracted from different regions of the AFM scan. Right: Height profile of the dye film coated on MoO_3 hole transport layer.

Organic Photovoltaic Device Fabrication

Used Architecture of the Organic Photovoltaic (OPV) Device

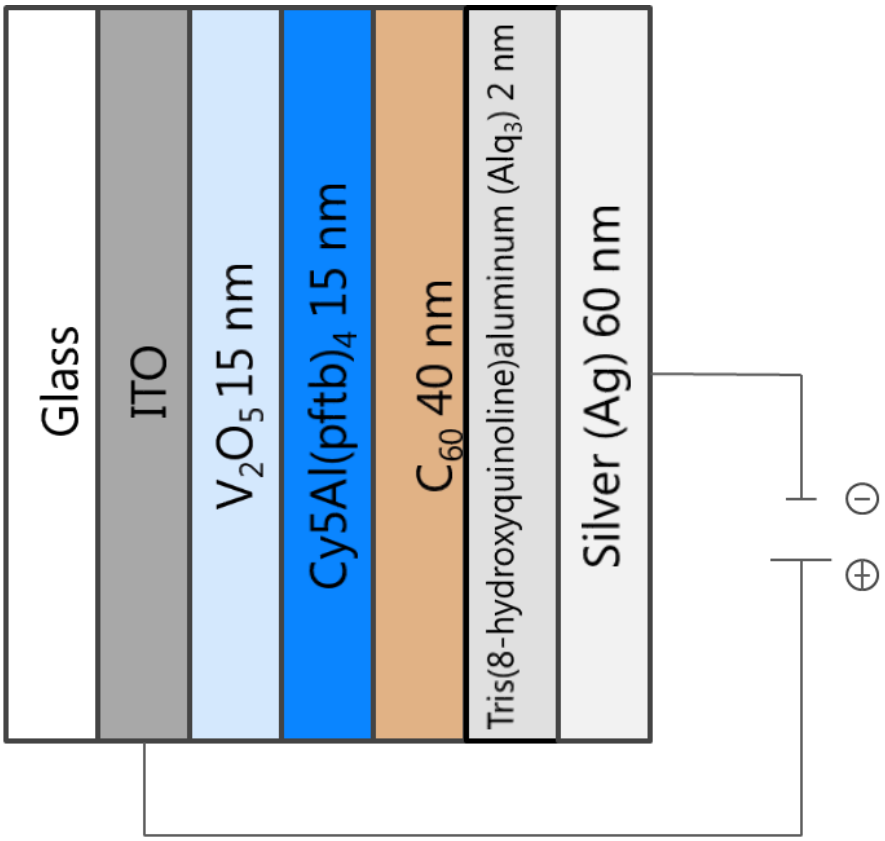

Figure S6. A sketch of the organic photovoltaic device architecture.

Active Layer Thickness Adjustment

Four concentrations of Cy5[Al(pftb)$_4$] ethanol solution were prepared and spincast at 4000 rpm for 1 min on 15 nm V_2O_5 hole transport layer. Subsequently all samples were analysed by ellipsometry. The obtained thicknesses were plotted against concentration to determine the correlation between thickness and concentration.

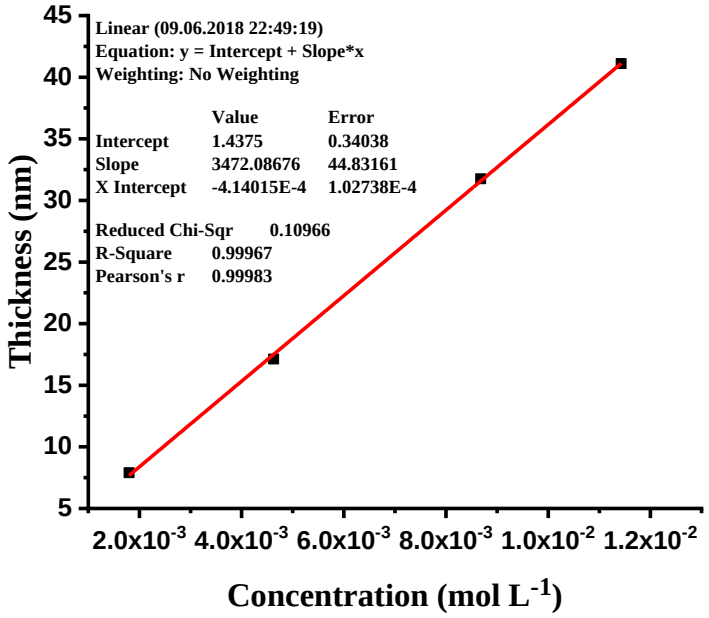

Figure S7. Correlation between concentration and resulting active layer thickness.

Therefore all necessary concentrations for any desired active layer thicknesses can be determined form the resulting linear equation fit.

Determination of Optimum Hole Transport Layer (HTL) Thickness

Optimum V_2O_5 interlayer thickness was adjusted using fixed 10 nm thick Cy5[Al(pftb)$_4$] layer while varying V_2O_5 thicknesses by 5, 10, 15, 20 and 30 nm. V_2O_5 was thermally deposited on ITO substrates.

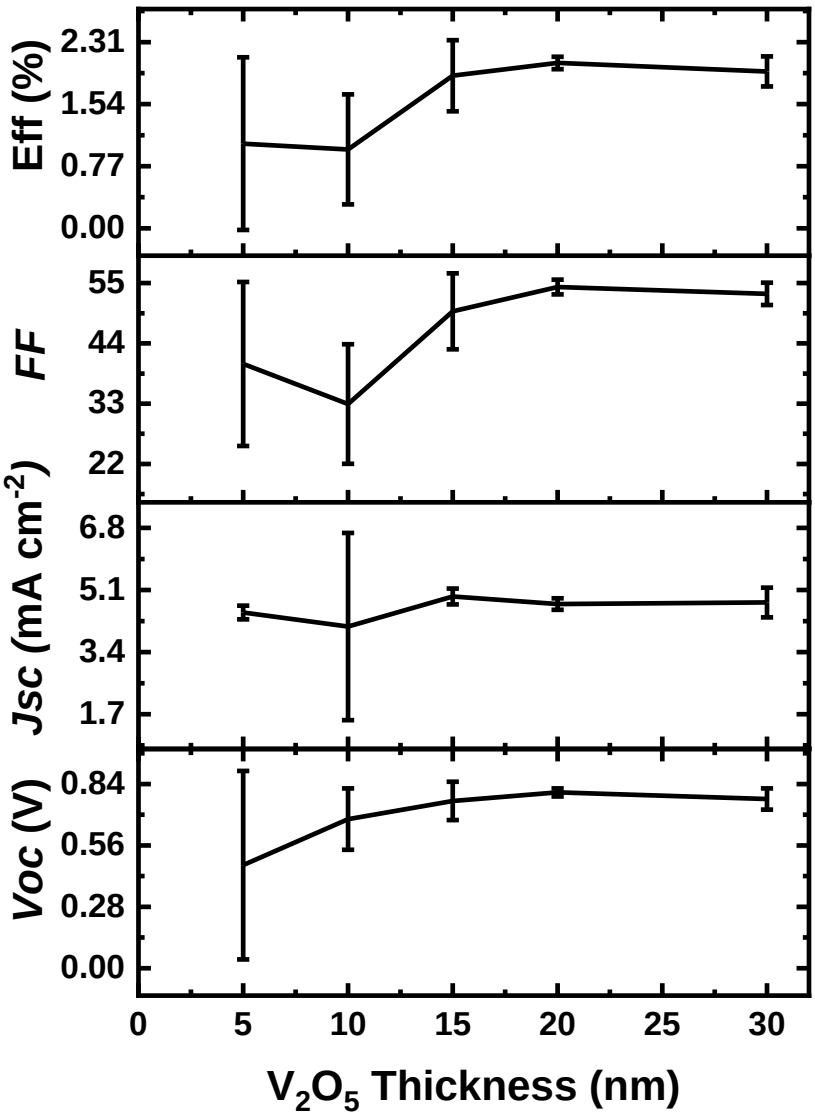

Figure S8. V_2O_5 thickness vs. JV parameters. Each data point represents averaged values from 8 cells with the corresponding standard deviation.

Thin V_2O_5 layers cause broad standard deviations, which are suppressed at thicker values. All parameters reach their plateau at around 20 nm V_2O_5 thickness. Values exceeding 20 nm V_2O_5 layer thickness cause a slight decrease in all OPV descriptive parameters. Therefore the obtained data indicates 15 nm of V_2O_5 as the optimum hole transport layer thickness with the highest potential for highest obtainable OPV device parameter values.

Determination of Optimum Active Light Absorbing Layer Thickness

After choosing 15 nm as the optimum thickness for the V_2O_5 HTL, the next step was to optimize the active light absorbing layer thickness by depositing 5, 10, 15, 20 and 30 nm of Cy5[Al(pftb)$_4$] on the HTL.

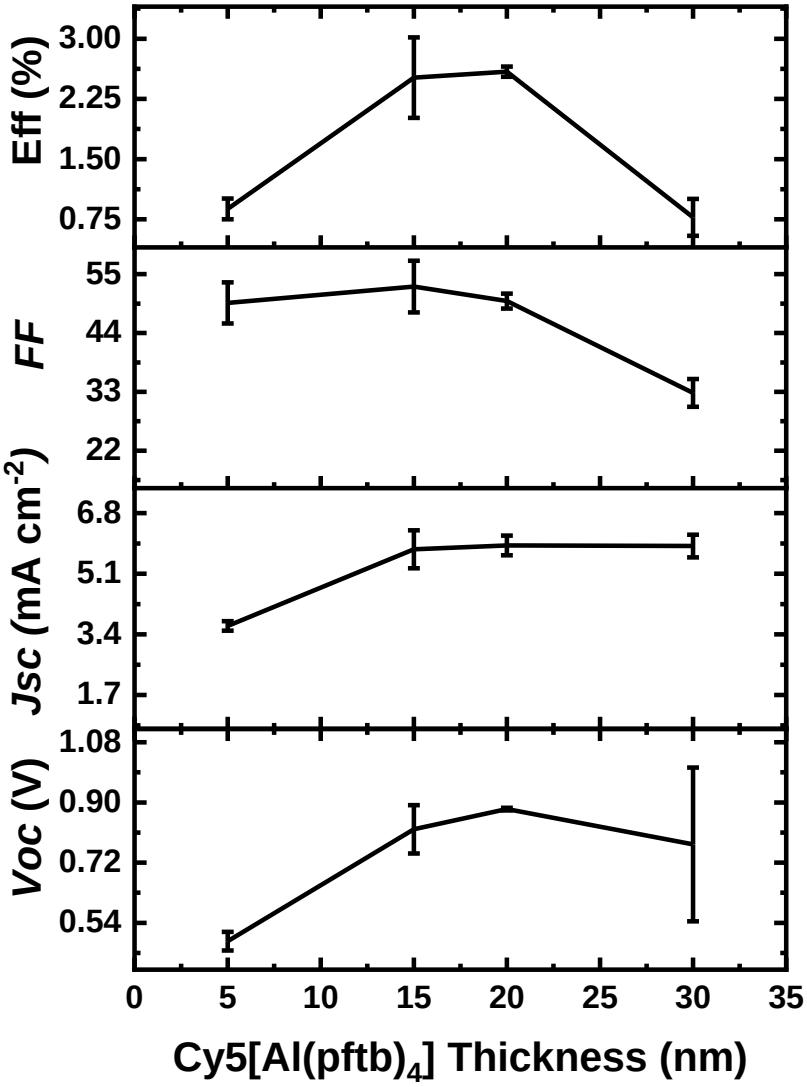

Figure S9. Cy5[Al(pftb)$_4$] thickness vs. JV parameters. Each data point represents averaged values from 8 cells with the corresponding standard deviation.

All descriptive OPV parameters rise with increasing active layer thicknesses and saturate at 15-20 nm. Thicker Cy5[Al(pftb)$_4$] layers cause a significant drop in all descriptive

parameters. 15 nm seems to be the optimum Cy5[Al(pftb)$_4$] thickness with the highest potential for this device configuration.

Optimized Device Descriptive Statistics

The fabrication of the final optimized devices was performed under consideration of the previously determined optimum interlayer thicknesses. Additionally new evaporation boats with freshly loaded material were used. The electrodes inside the evaporation chamber were cleaned by applying high current until all residual material was evaporated as monitored by a quartz sensor. The Cy5[Al(pftb)$_4$] was recrystallized from *t*BuOH and dried for two days at 3×10^{-3} mbar. The final transfer into the glovebox was carried out under vacuum.

Table S9. Descriptive statistics of the optimized Cy5[Al(pftb)$_4$] cells.

	N	$\bar{x}_{arithm}$	s	min	$\bar{x}_{med}$	max
V_{OC}/V	21	0.86	0.02	0.82	0.87	0.89
J_{SC}/mA cm^{-2}	21	6.17	0.43	5.63	6.06	7.23
η	21	3.22	0.23	2.91	3.15	3.79
FF	21	60.41	0.97	58.48	60.28	62.15

Short Circuit Current Density Calculation

The short circuit current density $J_{sc} = \int EQE(\lambda) \times \Phi_{AM1.5}(\lambda) \times e \, d\lambda$ was obtained by integrating over $EQE(\lambda)$, the photon flux $\Phi_{AM1.5}(\lambda)$ of the AM1.5 solar spectrum and multiplying by the elementary charge *e*.

Relative Permittivity

$$\varepsilon_r = n^2 - k^2$$

ε_r: relative permittivity (dielectric constant or function), n: real part of the index of refraction, k. imaginary part of the index (extinction coefficient)

The orientational polarization or dipole polarisation appears at low frequencies around 10^4 Hz. The n and k values are dependent on the wavelength. At higher wavelengths however the slope is very low and at a certain wavelength the k value becomes practically 0.

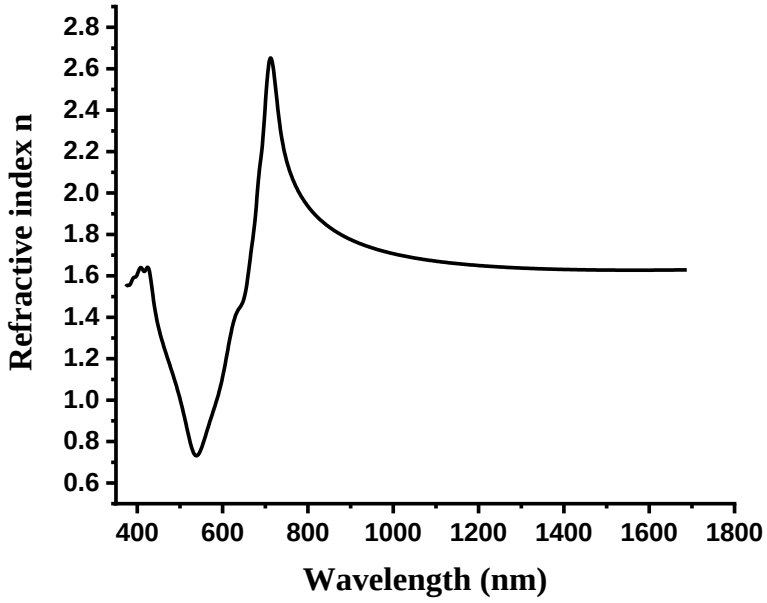

Figure S10. Function of n depending on the wavelength.

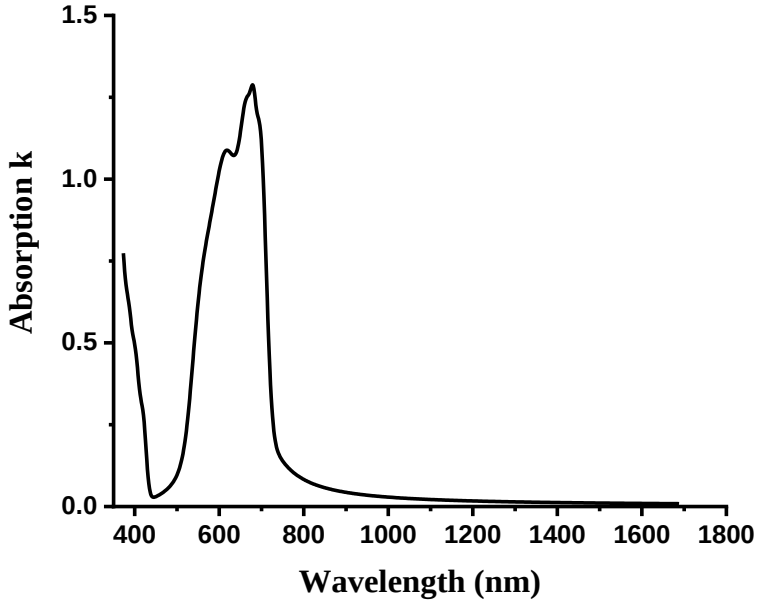

Figure S11. Absorption coefficient k depending on the wavelength.

Therefore this area was chosen for the calculation of the low frequence dielectric constant. The n are given in this table as averaged values over the selected wavelength region.

Table S10. Calculated relative permittivity values for the Cy5[Al(pftb)$_4$].

Cyanine	n	λ/nm	ε_r
Cy5[Al(pftb)$_4$]	1.64	1000-1688	2.68

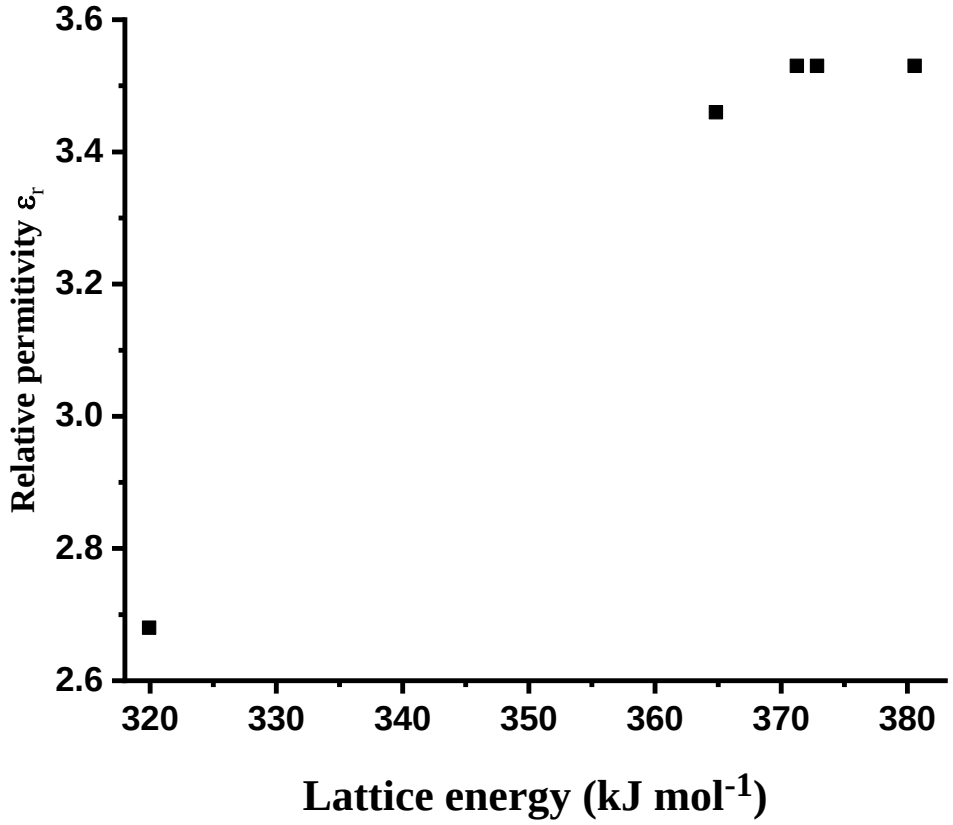

Figure S12. Relative permittivity as function of lattice energy of various Cy5 chromophore salts.

Literature

[1] H. D. B. Jenkins, H. K. Roobottom, J. Passmore, L. Glasser, *Inorg. Chem.* **1999,** *38,* 3609.

[2] O. V. Dolomanov, L. J. Bourhis, R. J. Gildea, J. A. K. Howard, H. Puschmann, *IUCr, J. Appl. Crystallogr.* **2009,** *42*, 339.

[3] G. M. Sheldrick, *Acta Crystallogr. Sect. C Struct. Chem.* **2015**, *71*, 3; G. M. Sheldrick, *Acta Cryst.* **2008,** *A64*, 112-122; A. L. Spek, *J. Appl. Cryst.* **2003,** *36,* 7-13.